String mechanism for the leading charm effect

C. E. Aguiar,[1] T. Kodama,[1] R. A. M. S. Nazareth,[1] and G. Pech[2]
[1]*Instituto de Física, Universidade Federal do Rio de Janeiro, C.P. 68528, 21945-970, Rio de Janeiro, Brazil*
[2]*Instituto de Física, Universidade do Estado do Rio de Janeiro, 20550-013, Rio de Janeiro, Brazil*
(Received 22 August 1997)

We argue that the leading charm effect observed in pion-nucleon interactions indicates the presence of rather strong color fields in hadronic collisions. We show that a flux tube picture which includes such strong fields accounts naturally for the leading charm phenomenon, providing a unified description of the production of charmed and noncharmed leading particles. [S0556-2813(98)00702-X]

PACS number(s): 24.85.+p, 13.85.Ni, 12.38.Lg, 25.75.Dw

I. INTRODUCTION

It is a general idea that the hadroproduction of heavy flavors is essentially a perturbative QCD (PQCD) process because of the large momentum transfer involved. In the case of charm, however, the quark mass is not large enough for PQCD calculations to be simply granted *a priori*. In fact, some experimental results indicate that nonperturbative processes play an important role in charm production. For example, in a pure PQCD picture the $c\bar{c}$ pairs are produced mainly with opposite p_T, due to the momentum conservation in parton-parton collisions. The observed transverse momentum distribution of the charmed pair shows almost no such back-to-back correlations [1]. In this case, however, one can still think of mechanisms that smear out the momentum correlation of the charm quarks during the hadronization process.

A more clear experimental indication for the existence of nonperturbative mechanisms of charm production is the leading charm effect [2], the strong flavor correlations that are observed between fast charmed hadrons and the beam particles. Recent high-statistics experiments, WA82 at CERN [3] and E769/E791 at Fermilab [4,5], have shown that in $\pi^{\pm}N\rightarrow D^{\pm}X$ reactions the x_F spectrum of leading D mesons is significantly harder than that of nonleading ones. By definition, a leading charmed meson is one that shares a valence quark with the projectile. With a π^- beam (as in the WA82 experiment) the incident quark content is $\bar{u}d$, so that $D^-(c\bar{d})$ is leading and $D^+(\bar{c}d)$ nonleading. A useful measure of the leading charm effect is the production asymmetry

$$\mathcal{A}(x_F)=\frac{\sigma_{\text{leading}}(x_F)-\sigma_{\text{nonleading}}(x_F)}{\sigma_{\text{leading}}(x_F)+\sigma_{\text{nonleading}}(x_F)}, \tag{1}$$

where σ_{leading} and $\sigma_{\text{nonleading}}$ are the cross sections for the leading and nonleading charmed particles as functions of Feynman's x_F. All experiments find that the asymmetry increases from $\mathcal{A}\simeq 0$ at $x_F\simeq 0$ to $\mathcal{A}\simeq 0.6$ at $x_F\simeq 0.7$. This large leading-nonleading asymmetry in the forward direction is very hard to understand in the PQCD scenario. A pure perturbative calculation predicts a much smaller effect ($\mathcal{A}<0.1$) [6].

The PQCD picture of leading charm production requires the introduction of some *ad hoc* mechanism that makes it possible for the charmed quarks, which are produced mainly in the central region, to coalesce with the fast moving beam quarks. An alternative approach, and perhaps a more natural one, is to consider that it is the very process of hadronization of the beam quarks that produces the charmed quarks they adhere to. This is actually the case for the leading particles of light flavors in the standard string models. In these models hadrons are produced via the breakup of strings extended between quarks of the projectile and target. The fastest moving particles come from the end point string fragments, those containing the valence quarks of the incident hadrons. This leads to strong flavor correlations between fast hadrons and the projectile. Unfortunately these models exclude the leading charm production, since in most standard string models the $c\bar{c}$ pair production rate is negligible.

In this paper we point out that the leading charm effect is naturally obtained in a string model, as long as one allows for color fields much stronger than that of a quark-antiquark string. In this way a general description of the production of leading particles, including charmed ones, can be achieved within the string picture. In previous works, we have in fact shown that introduction of such strong fields enables one to devise a string model (the ''firetube'' model of Refs. [7–10]) that describes rather well the production of charmed and noncharmed hadrons within a universal scheme. We argue that the observation of the leading charm effect could thus be considered as an indication that these very intense fields are present in hadronic collisions.

Other nonperturbative mechanisms have been proposed to explain the leading charm effect, and could in principle be added to the one considered here. These include intrinsic charm [11], valons [12], and the final state interaction between the (perturbatively produced) c quarks and beam remnants as implemented in PYTHIA [13].

In the following, we discuss the application of the firetube model to the production of leading particles in pp and πp collisions. In Sec. II we describe briefly the basic ideas of the firetube model. In Sec. III the production of leading particles (not necessarily charmed) is discussed, and the momentum distributions of leading protons and Λ's produced in pp collisions are calculated and compared to data. The D mesons produced in πN interactions and the leading charm effect are discussed in Sec. IV. A summary and conclusions are presented in Sec. V.

II. FIRETUBE MODEL

The firetube model is a combination of the string and statistical approaches to particle production in hadronic collisions. In this section we give only a rapid description of the model; more details can be found in Refs. [7–10]. The basic idea of the model is that the two colliding hadrons exchange gluons as they pass by each other, acquiring color charges $\pm Q$ in the process (we omit the color SU_3 indices for simplicity). A flux tube is formed between the receding particles, confining the chromoelectric field created by their color charges. This tube is represented as a single effective one-dimensional classical string with a tension k proportional to the energy density of the chromoelectric field. Because of the multiple exchange of gluons, the color structure at the end points of the tube is more complicated than that of an ''elementary'' color-triplet $q\bar{q}$ string (for example, that generated in the electron-positron annihilation process). If the radius of the flux tube is independent of the color charge at the end points, as suggested by lattice QCD calculations [14], the string tension depends upon Q as

$$k = k_0 Q^2, \tag{2}$$

where k_0 is the tension of a $q\bar{q}$ string (we take $Q=1$ as the quark color charge). The color charge Q fluctuates from one collision to another because different numbers of gluons may be exchanged, and also because of the SU_3 rules of color addition. Assuming that each gluon exchange is a step of a random walk in color space [15], the mean end point charge is given by

$$\overline{Q^2} = \tfrac{9}{4}\bar{n}, \tag{3}$$

where $\bar{n}$ is the average number of exchanged gluons. It is clear from Eqs. (2) and (3) that the exchange of even a few gluons generates string tensions significantly larger than that of a $q\bar{q}$ string.

The motion of the two colored particles at the string end points is given by the classical equations

$$\frac{dp_i}{dt} = \mp k, \tag{4}$$

$$\frac{dx_i}{dt} = \frac{p_i}{\sqrt{p_i^2 + m_i^2}}, \tag{5}$$

where x_i and p_i $(i=1,2)$ are the coordinates and momenta along the string direction. The minus (plus) sign in Eq. (4) applies when particle i is to the right (left) of its partner. In the center-of-mass frame, the trajectories of the end point particles are given by branches of hyperbolas

$$\left(x_i \mp \frac{\sqrt{s}}{2k}\right)^2 - \left(t_i - \frac{\sqrt{s}}{2k}\right)^2 = \left(\frac{m_i}{k}\right)^2. \tag{6}$$

The m_i appearing in Eqs. (5) and (6) are not the masses of the projectile and target. We assume that the incoming particles are excited by the collision, and that m_i, the masses of the resulting colored systems, are given by $m_i = M_i + \mu$, where M_i is a minimum value and μ has a Gaussian probability distribution $\exp(-\mu^2/2\sigma_m^2)$. We take σ_m to be proportional to the number of gluons exchanged, $\sigma_m = n_{\text{gluons}}\Delta m$, Δm being a parameter of the model. For M_i we use the mass of the corresponding incident particle plus that of a pion.

The chromoelectric field inside the tube produces quark-antiquark pairs by a process similar to the Schwinger mechanism of electron-positron creation in QED [16]. The production rate of $q\bar{q}$ pairs per unit volume and unit time can be calculated (in the Abelian approximation) from Schwinger's formula

$$\mathcal{R}_q = \frac{F^2}{4\pi^3}\sum_{n=1}^{\infty}\frac{1}{n^2}\exp(-n\pi m_q^2/F), \tag{7}$$

where $F = 2k_0 Q$ is the chromoelectric force that a quark feels inside the tube, and m_q is the quark mass. In our calculations we have modified Eq. (7) in order to account for the final state interaction of the $q\bar{q}$ system and the finite size of the flux tube [17–19].

The quarks pairs created by the chromoelectric field tend to screen the end point charges Q. This screening makes it possible for the flux tube to break up into two pieces once Q pairs have been produced inside it. A simple estimate for the flux tube fragmentation rate per unit length per unit time is then obtained as

$$\frac{dP}{dx\,dt} = \frac{S\mathcal{R}}{Q}, \tag{8}$$

where S is the cross section area of the tube, and $\mathcal{R} = \mathcal{R}_u + \mathcal{R}_d + \mathcal{R}_s + \cdots$ is the total number of quarks produced per unit volume and unit time. We assume that the flux tube breaks up according to the Artru-Mennessier area law [20] (see Ref. [21] for an alternative approach), and the resulting fragments are regarded as clusters of excited hadronic matter, or ''fireballs,'' which decay statistically into the observed hadrons. The temperature of a fireball is determined by its mass, being typically of the order 100 MeV. The fireballs can have strangeness or charm, if one of the s or c quarks produced by the color field happens to be captured inside it during the fragmentation process. In this case the mesons produced by the fireball thermal decay will include a K or a D.

The firetube model has a small number of parameters. The most important one is the mean color charge $\overline{Q^2}$ or, alternatively, the average number of gluons exchanged per collision, $\bar{n}$. Other relevant parameters are the elementary string constant k_0, the flux tube cross section S, and the leading-fragment excitation parameter Δm. Finally, a few constants define the minimum fireball mass, and determine how the effective temperature and longitudinal expansion rate of a fireball depend upon its mass. For proton-proton collisions we use $\bar{n} = 2.0$, $k_0 = 1$ GeV/fm, $S = 1.5$ fm^2, and $\Delta m = 0.3$ GeV, obtaining a very good description of the momentum distributions of pions, kaons, and D's [7]. For pion-nucleon collisions the only changes in this parameter set are $\bar{n} = 2.5$ and $\Delta m = 0.6$ GeV.

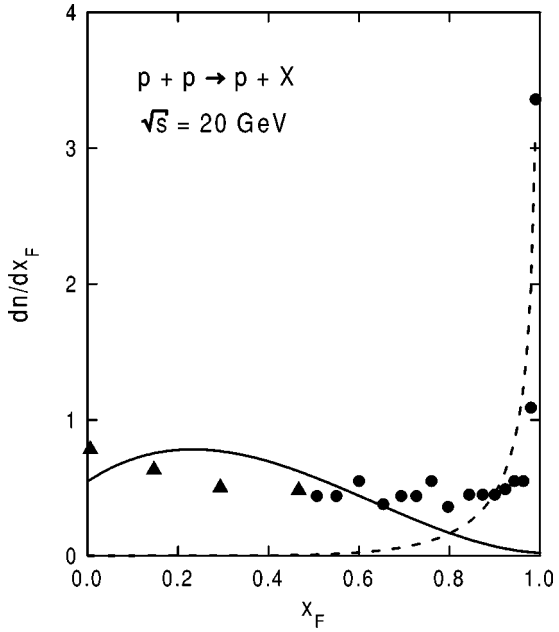

FIG. 1. x_F spectrum of protons from pp collisions. Triangles and circles refer to different experiments [22,23]. The solid line is the firetube model calculation. The dashed line is the diffractive cross section.

III. LEADING PARTICLE SPECTRA

The leading nucleons produced in proton-proton collisions have a fairly flat x_F distribution. This experimental observation is better reproduced if we assume that the extremities of the flux tube, which carry the projectile and target remnants, detach from the string at space-time points distributed (in the c.m. frame) according to

$$\frac{d^2P_i}{dxdt}=2\delta[(x\mp t_0)^2-(t-t_0)^2-(m_i/k)^2], \tag{9}$$

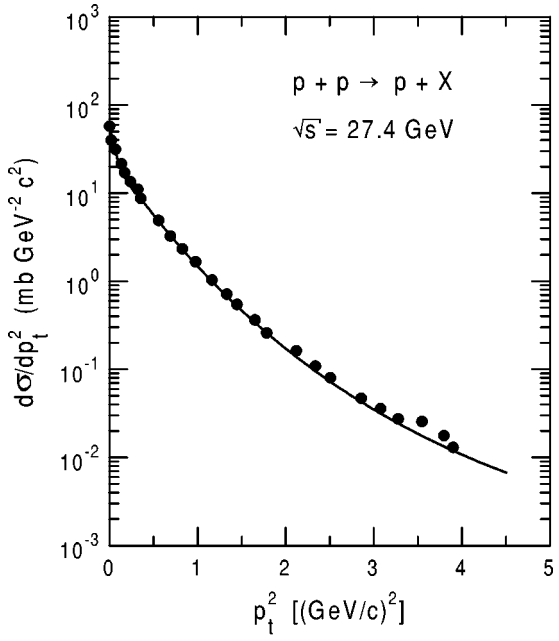

FIG. 2. $p_T{}^2$ spectrum of protons from pp inelastic collisions. Experimental data is from Ref. [24]. The solid line is the firetube model calculation.

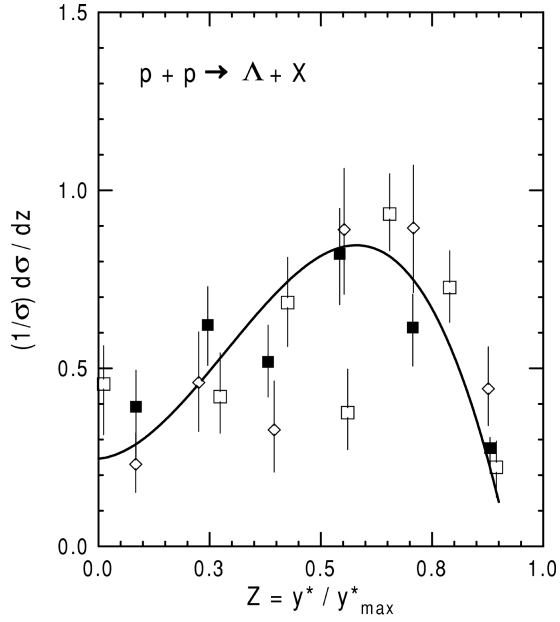

FIG. 3. c.m. rapidity distribution of Λ hyperons produced in pp collisions. Open squares indicate data taken at 200 GeV/c [25]; open diamonds and black squares are from different experiments at 300 GeV/c [26,27]. The solid line is the firetube model result.

where $t_0=\sqrt{s}/(2k)$, and the argument of the δ function is the trajectory of the end point particles [see Eq. (6) and the corresponding sign conventions]. The distribution of the leading fragment break points does not follow the uniform space-time density of internal string ruptures given in Eq. (8), but this is not surprising since the more complex structures at the end points of the flux tube should affect somehow the detaching mechanism. The time distribution of leading break points can be written

$$\frac{dP_i}{dt}=\frac{1}{\lambda_i(t)}, \tag{10}$$

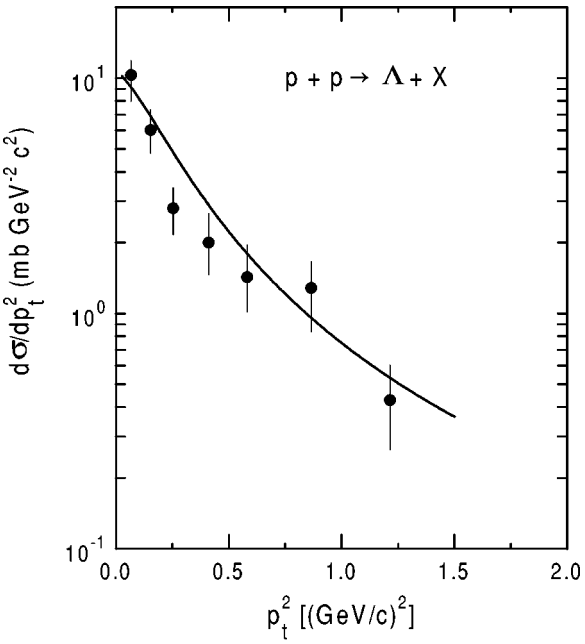

FIG. 4. $p_T{}^2$ spectrum of Λ hyperons produced in pp collisions at 205 GeV/c [25]. The solid line is the firetube model calculation.

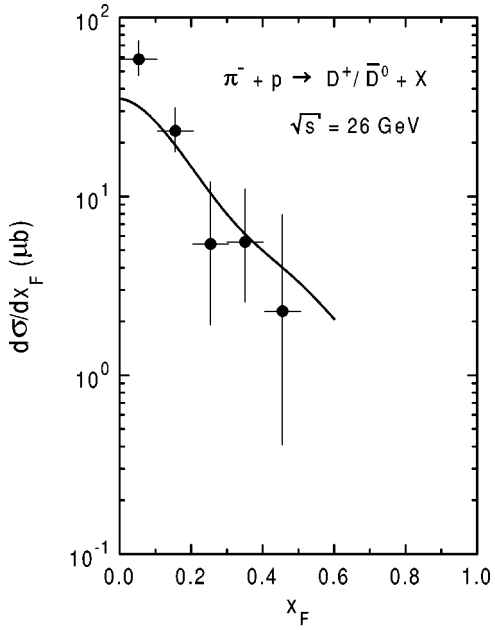

FIG. 5. The distribution in x_F for nonleading $(D^+/\overline{D^0})$ mesons. The solid curve is the firetube model prediction. Experimental points are from Ref. [2].

where (in the c.m. frame) $\lambda_i(t)=\sqrt{(t-t_0)^2+(m_i/k)^2}$. The probability density for the detaching to occur at t is then

$$\mathcal{P}_i(t)=\frac{1}{\lambda_i(t)}\exp\left(-\int_{t_c}^{t}\frac{dt'}{\lambda_i(t')}\right)=\frac{1}{\lambda_i(t)}\,\frac{t_c-t_0+\lambda_i(t_c)}{t-t_0+\lambda_i(t)}, \tag{11}$$

where t_c is the collision time $[x_1(t_c)=x_2(t_c)]$.

In high-energy collisions we have $\sqrt{s}\gg m_i$ and $\mathcal{P}(t)\simeq 1/t_0$, a constant probability distribution for $0<t<t_0$.

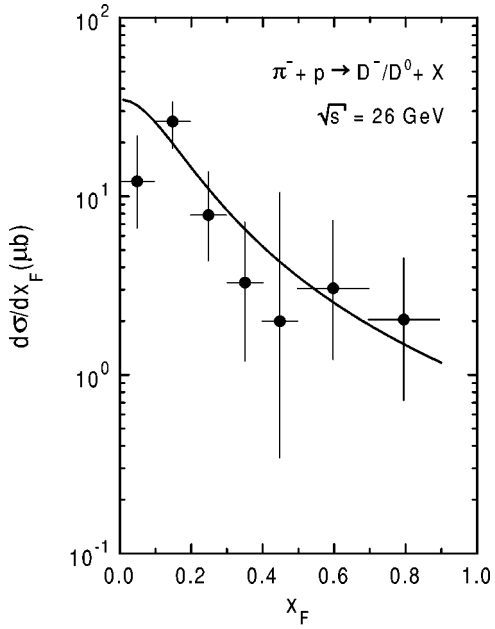

FIG. 6. The distribution in x_F for leading (D^-/D^0) mesons. The solid curve is the firetube model prediction. Experimental points are from Ref. [2].

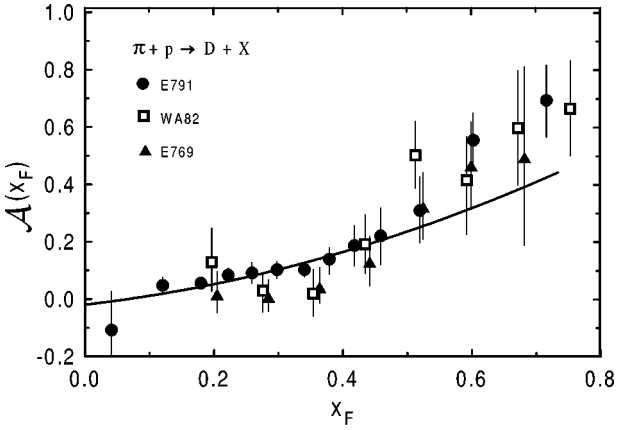

FIG. 7. The charged D production asymmetry $\mathcal{A}$ as a function of x_F. The solid curve corresponds to the firetube model calculation. The experimental data are from the WA82 [3], E769 [4], and E791 [5] Collaborations.

Since the momentum of the end point particles is linearly related to the time t, such a $\mathcal{P}(t)$ gives rise to a homogeneous longitudinal momentum distribution of the leading fragments. We assume that each fragment decays into two leading particles, both carrying valence quarks that originally belonged to the beam. One of these particles is typically a pion. The other is the leading baryon or meson we are interested in or a low-lying excitation of it. There is a finite probability that the end point fragments carry strangeness or charm. This is because the color screening that occurs during the detaching process should involve to some extent the quarks produced inside the flux tube, and these include strange and charmed ones. We consider the fraction $\mathcal{R}_{s,c}/\mathcal{R}$ to be the probability that a leading fragment carries a strange or charmed quark. $\mathcal{R}_{s,c}$ is the strangeness or charm creation rate as given by Eq. (7), and $\mathcal{R}$ denotes the total quark production rate as used in Eq. (8).

In Fig. 1 we show the x_F spectrum of protons from pp reactions at $\sqrt{s}=20$ GeV. For $0<x_F<0.7$ the model calculation (solid line) is in reasonable agreement with the data [22,23]. At larger values of x_F the cross section for diffractive dissociation becomes important (dashed line). If this is added to our calculation, we see that a good overall agree-

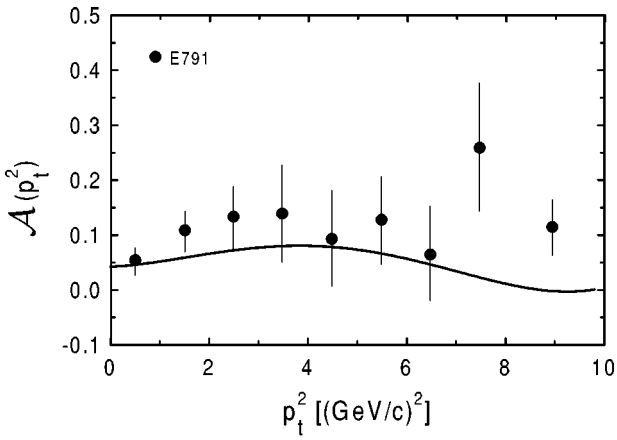

FIG. 8. The charged D production asymmetry $\mathcal{A}$ as a function of p_T. The solid curve corresponds to the model calculation. The experimental points are from Ref. [5].

ment with the experimental data is achieved. The transverse momentum distribution of protons from pp inelastic collisions at $p_{\rm lab}=400$ GeV/c is shown in Fig. 2. The calculation follows quite well the experimental distribution [24].

In Fig. 3 we show the rapidity distribution of Λ hyperons produced in pp collisions. A good agreement is found between the model calculations and the experimental data [25–27]. The transverse momentum distribution we obtain for the Λ is also in accordance with the experimental results [25], as seen in Fig. 4.

IV. LEADING CHARM EFFECT

We now discuss in detail the leading charm effect observed in πN interactions. In applying the firetube model to charm production, we assume that only D and D^* mesons come out of the charmed fireballs, and that their relative number is given by the multiplicity of spin states, $D^*/D=3$. Considering for definiteness that the beam particle is a π^-, the cross sections for the production of the different D mesons are

$$\sigma_{D^-}=0.122\sigma^{(C)}+0.244\sigma^{(L)}, \tag{12}$$

$$\sigma_{D^+}=0.122\sigma^{(C)}, \tag{13}$$

$$\sigma_{D^0}=0.378\sigma^{(C)}+0.500\sigma^{(L)}, \tag{14}$$

$$\sigma_{\overline{D^0}}=0.378\sigma^{(C)}+0.256\sigma^{(L)}, \tag{15}$$

where $\sigma^{(C)}$ is the fraction of the total charm cross section associated with the mesons that come out of the central fireballs, and $\sigma^{(L)}$ is the corresponding fraction for the end point (leading) fragments. Note that nonleading $\overline{D^0}$ mesons may originate from the decay of a leading D^{*-}. This explains the $\sigma^{(L)}$ contribution to the $\overline{D^0}$ cross section.

In Figs. 5 and 6 we show the x_F distribution of nonleading $(D^+/\overline{D^0})$ and leading (D^-/D^0) charmed mesons produced in $\pi^- p$ reactions at 360 GeV/c. We note the harder spectrum of the leading particles and the good agreement between the calculations and the experimental data [2].

Written in terms of $\sigma^{(L,C)}$, the $D^\pm$ production asymmetry measured by the WA82 and E769/E791 Collaborations has the simple form

$$\mathcal{A}=\frac{\sigma^{(L)}}{\sigma^{(C)}+\sigma^{(L)}}. \tag{16}$$

In Fig. 7 we compare this asymmetry, calculated as a function of x_F, with the experimental results [3–5]. The overall agreement is good, although we tend to underestimate the data at large x_F. The asymmetry $\mathcal{A}$ as a function of the transverse momentum is shown in Fig. 8. The calculation follows reasonably well the recent experimental data of E791, except in the high-p_T region.

V. SUMMARY

Leading particle effects appear naturally in soft hadronization schemes like string models. The usual string models fail to describe the leading charm effect only because they predict that no charm is produced by the fragmentation process. This is not the case with the firetube model, which is based on the idea that a single flux tube confining a very strong color field is formed between the colliding hadrons after they pass by each other. The tension of the tube is larger than the usual triplet-antitriplet string tension, and may reach values at which even $c\overline{c}$ pairs are produced at significant rates. This gives a simple explanation for the leading charm effect: A $c\overline{c}$ pair that contributes to the screening of the end point color charge will have one of its quarks carried out by the leading fragment, which also contains the original valence quarks of the beam particle. The decay of this fragment gives rise to the flavor correlations that characterize the leading charm effect.

The results of this work show that such a framework is able to account for the main features of the leading charm effect, providing a unified view of all leading particle phenomena.

[1] K. Kodama *et al.*, Phys. Lett. B **263**, 579 (1991); S. Oaki *et al.*, Prog. Theor. Phys. **87**, 1305 (1992); S. Barlag *et al.*, Phys. Lett. B **302**, 112 (1993); M. Adamovich *et al.*, CERN Report No. CERN/PPE 94-214, 1994.

[2] M. Aguilar-Benitez *et al.*, Phys. Lett. **161B**, 400 (1985).

[3] M. Adamovich *et al.*, Phys. Lett. B **305**, 402 (1993).

[4] G. A. Alves *et al.*, Phys. Rev. Lett. **72**, 812 (1994).

[5] E. M. Aitala *et al.*, Phys. Lett. B **371**, 157 (1996).

[6] P. Nason, S. Dawson, and R. K. Ellis, Nucl. Phys. **B327**, 49 (1989).

[7] C. E. Aguiar, T. Kodama, R. A. M. S. Nazareth, and G. Pech, Phys. Rev. C **53**, 448 (1996).

[8] N. Prado, R. A. M. S. Nazareth, and T. Kodama, Rev. Bras. Fis. **16**, 452 (1986).

[9] R. A. M. S. Nazareth, N. Prado, and T. Kodama, Phys. Rev. D **40**, 2861 (1989).

[10] R. A. M. S. Nazareth, T. Kodama, and D. A. Portes, Phys. Rev. D **46**, 2896 (1992).

[11] R. Vogt and S. Brodsky, Nucl. Phys. **B438**, 261 (1995).

[12] R. W. Hwa, Phys. Rev. D **51**, 85 (1995).

[13] H.-U. Bengtsson and T. Sjöstrand, Comput. Phys. Commun. **46**, 43 (1987).

[14] N. A. Campbell, I. H. Jorysz, and C. Michael, Phys. Lett. **169B**, 91 (1986); H. D. Trottier and R. M. Woloshin, Phys. Rev. D **48**, 2290 (1993).

[15] T. S. Biro, H. B. Nielsen, and J. Knoll, Nucl. Phys. **B245**, 449 (1984).

[16] J. Schwinger, *Particles, Sources and Fields* (Addison-Wesley, Reading, MA, 1973).

[17] C. Martin and D. Vautherin, Phys. Rev. D **40**, 1667 (1989).

[18] H.-P. Pavel and D. M. Brink, Z. Phys. C **51**, 119 (1991).

[19] C.-Y. Wong, R.-C. Wang, and J.-S. Wu, Phys. Rev. D **51**, 3940 (1995); R.-C. Wang and C.-Y. Wong, *ibid.* **38**, 348 (1998).
[20] X. Artru and G. Mennessier, Nucl. Phys. **B70**, 93 (1971).
[21] L. Wilets and R. D. Puff, Phys. Rev. C **51**, 339 (1995).
[22] P. Cappiluti *et al.*, Nucl. Phys. **B70**, 1 (1974).
[23] J. W. Chapman *et al.*, Phys. Rev. Lett. **32**, 257 (1974).
[24] Aguilar-Benitez *et al.*, Z. Phys. C **50**, 403 (1991).
[25] K. Jaeger, D. Colley, L. Hyman, and J. Rest, Phys. Rev. D **11**, 2405 (1975).
[26] A. Sheng *et al.*, Phys. Rev. D **11**, 1733 (1991).
[27] F. LoPinto *et al.*, Phys. Rev. D **22**, 573 (1980).